Chen, H and Qian, L and Ma, Z and Causon, D and Mingham, C (2018)*Numerical simulation of phase-focused wave group interaction with an FPSO-shaped body.* In: International Ocean and Polar Engineering Conference, 10 June 2018 - 15 June 2018, Sapporo, Japan.

Numerical Simulation of Phase-Focused Wave Group Interaction with an FPSO-Shaped Body

Hao Chen, Ling Qian, Zhihua Ma, Derek Causon and Clive Mingham
School of Computing, Mathematics & Digital Technology
Manchester Metropolitan University, Manchester, UK

ABSTRACT

The present paper summarizes the results for numerical simulation of a fixed FPSO-shaped body in uni-directional phase-focused wave groups, which is prepared as a short report for the CCP-WSI Blind Test Workshop on Focused Wave Impact on a Fixed FPSO at the 28th International Ocean and Polar Engineering Conference (ISOPE 2018). The numerical simulations were carried out using the open source toolbox OpenFOAM. An overset mesh method was applied, where two layers of mesh were generated, namely the background mesh and the overlapping body-fitted mesh. The incident focused wave groups were first validated against the experimental data at several positions. With the propagation of the waves, it was found that the waves generated by the numerical model were slightly dissipated due to numerical diffusion. Therefore, smaller wave crest was predicted from the numerical model. Then the simulations were conducted for the same wave conditions with the FPSO structure in place. The surface elevation and the pressure at several locations based on the validation criteria are reported.

KEY WORDS: focused wave group; hydrodynamic force; OpenFOAM; FPSO; overset grid.

INTRODUCTION

The floating production storage and offloading (FPSO) vessels are used in offshore oil and gas industry. They are usually operated in deep water conditions where harsh marine environment may be encountered. Therefore, it is of importance to examine the survivability of the FPSO in such extreme sea state.

Previously there have been several publications on extreme wave loads on fixed structures. Zang et al. (2006) presents the effects of second order wave diffraction in wave run-up around the bow of a vessel (FPSO) for regular waves and focused wave groups. Chen et al (2014) analysed the high order components of the wave load on a monopole. Paulsen et al. (2014) investigated numerically the forcing by steep regular water waves on a vertical circular cylinder at finite depth. Special attention was paid on the second load cycle. It was found that the second load cycle was caused by the strong nonlinear motion of the free surface, which drives a return flow at the back of the cylinder following the passage of the wave crest.

At COAST laboratory in Plymouth University, a series of experiments have been performed for wave interaction with simplified FPSO-shaped bodies to look into the scattered waves due to presence of FPSO. The effects of the model length, wave steepness and incident wave direction were investigated. The results were summarized and reported in Mai et al. (2016). Meanwhile, Hu et al. (2016) numerically reproduced the experiments using OpenFOAM. The numerical results compared well with the experimental data.

As part of the programmes at ISOPE 2018, the CCP-WSI Blind Test Workshop on Focused Wave Impact on a Fixed FPSO Model is being organised. The proposed benchmark cases are the same as described in Mai et al. (2016), but with different wave conditions. The purpose of the workshop is to evaluate the accuracy and efficiency of different numerical models for simulating wave-structure interaction, and provide insight on model fidelity for this particular flow problem. In the present work, we utilize the open source toolbox OpenFOAM to reproduce the benchmark experiments conducted at COAST laboratory. A two-phase free surface flow solver is applied to solve the incompressible Navier-Stokes equations. An overset grid method is applied to discretize the domain and to represent the solid object. The incident focus wave group is first generated in an empty 3D wave tank, which is validated against the experimental data provided by the CCP-WSI consortium. Then, the results are presented for wave interaction with the FPSO model under different wave conditions, which is followed by a brief summary of the work.

DESCRIPTION OF THE NUMERICAL MODEL

Free surface flow solver

The numerical model solves the incompressible Navier–Stokes equations for a two-phase flow of water and air with incorporation of a VOF scheme for tracking the free surface. The governing equations are given as:

$$\nabla \cdot u = 0 \tag{1}$$

$$\frac{\partial(\rho u)}{\partial t} + \nabla \cdot (\rho u)u = \nabla p - (g \cdot x)\nabla \rho + \nabla \cdot \mu(\nabla u) \tag{2}$$

$$\frac{\partial \alpha}{\partial t} + \nabla \cdot u\alpha + \nabla \cdot u_r \alpha(1-\alpha) = 0 \tag{3}$$

where $u=(u, v, w)$ is the velocity field in Cartesian coordinates, and g is the vector of gravity, ρ is density and μ is viscosity. They can be obtained from the volume fraction field as $\rho = \rho_w \, \alpha + \rho_a \, (1\text{-}\alpha)$, $\mu = \mu_w \, \alpha + \mu_a \, (1\text{-}\alpha)$, where ρ_w and μ_w are the density and viscosity of water, ρ_a and μ_a are the density and viscosity of air. The hydrodynamic pressure was applied in Eq. (2), where the hydrostatic pressure was subtracted. This can greatly ease the definition of boundary condition, and enhance the stability of the solver. Eq. (3) is the transport equation for volume fraction field α. In order to maintain the sharp interface and avoid smearing of it, OpenFOAM introduces an anti-diffusive term to compress the interface. The velocity field u_r is the so-called compressive velocity, which is only active at the interface. The details of this formulation can be referred to Márquez (2013).

Turbulence model

For this particular test case, turbulent effects are not considered to be significant as the non-dimensional wave parameter (wave steepness) k_pA is smaller than 3 (k_p is the wavenumber at spectral peak frequency, A is the crest height of the focused wave group) and we do not expect wave breaking to occur. However, we have applied a commonly used k-ω SST model in the simulation, since the Reynolds number may still be large enough to generate turbulent wake behind the FPSO. Nevertheless, we emphasize that the inertia effects are dominant and flow turbulence is expected to play a minor role in this benchmark test.

Numerical wave generation

The waves in the numerical wave tank were generated using IHFOAM, as introduced in Higuera et al. (2013). IHFOAM implements wave making boundary conditions by directly introducing flow flux into the computational domain based on the surface elevation and the velocity profile, which can be prescribed by users. In the present work, the applied velocity profile and surface elevation were calculated by a second order uni-directional focused wave theory. The detailed formulation can be found in Hu et al. (2016) and Ning et al. (2009). The amplitudes, wave numbers and frequencies of each wave component were calculated based on the NewWave theory using the JONSWAP spectrum.

The second order wave theory actually contains wave-wave interaction between two wave components. It is an extension of the second order bi-chromatic wave theory. Essentially both surface elevation and velocity profile contain components whose frequencies are the summation and difference of these two components, and the summation of its own frequency. The transfer functions indicate the strength of the interactions between wave components. Although third order wave theory is also available (Madsen and Fuhrman (2006) and Madsen and

Fuhrman (2012)), it was not implemented. The reason is that the surface elevation and velocity profile are only for excitation of waves. By conducting some numerical tests, it was concluded that the computed surface elevation is not sensitive to the higher order wave components. Therefore, second order wave theory was applied for the blind test. This has also been confirmed in Hu et al. (2016).

NUMERICAL REPRODUCTION OF THE BLIND TEST

Description on the physical experiments

The physical experiments were performed at COAST laboratory in Plymouth University, UK. The tests were performed in the Ocean Basin, which has a length of 35 m and width of 15.5 m. A fixed FPSO scale-model was subjected to a series of focused wave events with a range of steepness, kA=0.13-0.21. The purpose of these experiments was to assess factors, such as wave steepness and (and direction, effecting the forces and run-up on FPSO hulls due to extreme wave events.

The test matrix is given in Table 1. For all the test conditions, the water depth was the same, i.e. 2.93 m. For the three cases considered they all have the constant (0°) angle of incidence but with increasing wave steepness. In the physical experiments, each wave group was created using linear superposition of 244 wave fronts with frequencies evenly spaced between 0.101563 Hz and 2 Hz. The FPSO was placed at the theoretical focus location, x_0=13.886 m downstream from the wave paddles. The amplitudes of the frequency components were derived by applying the NewWave theory to a JONSWAP spectrum with the parameters in the Table 1.

Table 1. The test matrix for the incoming focused wave groups in the experiments

Test ID	A [m]	Tp [s]	Hs [m]	Alpha [rad]	Phi [rad]
11BT1	0.06914	1.456	0.077	0	π
12BT1	0.09128	1.456	0.103	0	π
13BT1	0.09363	1.362	0.103	0	π

In the experiments for the empty wave tank test, the surface elevations at various positions were measured. For the test where the FPSO was in place, both the pressure and the surface elevations were measured. Readers are referred to the WSI-CCP website at http://www.ccp-wsi.ac.uk for detailed information on the setup of the experiments. As a blind test, the surface elevation in the empty tank has been released, as a priori known to the authors. The measured data with structure in place are not provided. In the following section, we will first validate the generated wave group in the empty wave tank against the released experimental data. Then we report the numerical results for the surface elevation and the pressure value from the wave tank with FPSO in place.

Computational domain and mesh

A series of 2D numerical experiments were first carried out to determine the domain length, focal position, focal time and mesh resolution. Eventually, the length of the numerical wave tank was set to 10 m, and the focal position was 3 m downstream from the wave-maker side and the focal time is 12 s. In the experiments, the ocean basin has a width of 15.5 m, which will reduce the blockage effects to a minimum. In the numerical tank, however, the width was shortened to 4 m, in

order to save the computational time. We applied an overset mesh grid for the numerical computation. A background mesh was generated first using the blockMesh utility. Then a body-fitted mesh was produced around the FPSO model by the snappyHexMesh utility. Essentially these two layers of mesh were merged together, and field values were interpolated between these two meshes. The total number of mesh cells including both background layer and body-fitted layer is 2.4 million, which has been demonstrated to be sufficient for convergent results. Fig. 1 presents an overview of the overset mesh, while Fig. 2 shows the details of the mesh at the overlapping area.
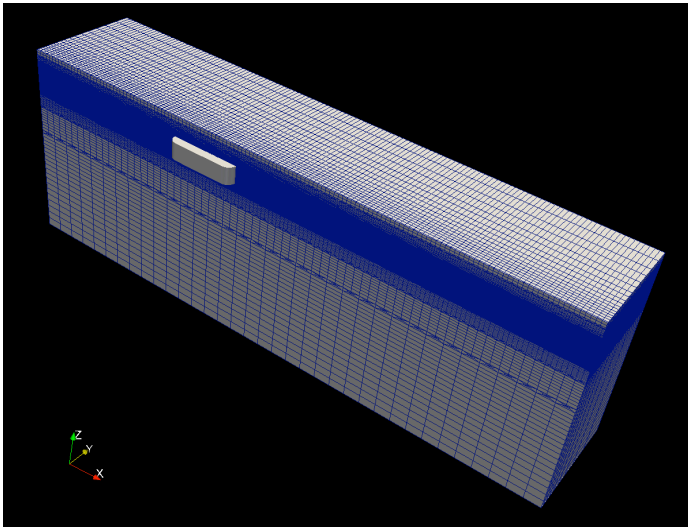
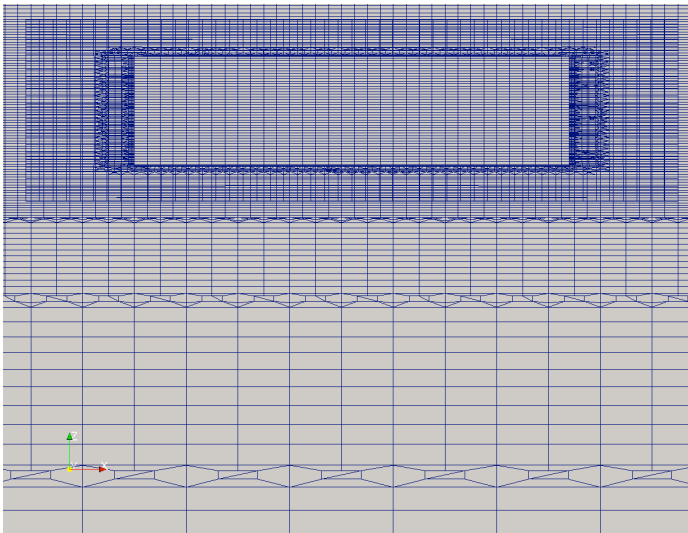Fig. 1 An overview of the mesh structure for the numerical wave tank with FPSO in place.

Fig. 2 The merged mesh at overlapping area.

Validation of the incident waves

In this section, we present the comparison between the numerical results and the experimental data from the empty wave tank tests. The locations of the wave gauges have been given in the WSI-CCP blind test website. We mainly compare the surface elevation at WG01 (front of the tank), WG04 (side of tank), WG08 (side of tank), WG14 (back of tank) and WG16 (focal position).

Fig. 3-5 presents the comparison of the surface elevation at these gauges. Some observations are given here: (1) In general, the agreement is satisfactory for all the cases. (2) At the back side of the numerical wave tank (WG14), we observe lower wave crest due to numerical diffusion. Actually, we applied Crank-Nicolson scheme for the time derivative term rather than the commonly used Euler scheme. This scheme could reduce the numerical diffusion effectively. However, it was not stable enough. This will be further seen in the next section. (3) The numerical diffusion becomes more significant for steeper waves (e.g. case 13BT1). (4) As the incident wave group is trough focused, two peaks with approximately equal crest was expected at WG 16, namely the theoretical focal position. However, the numerical model produces a smaller crest for the first peak.
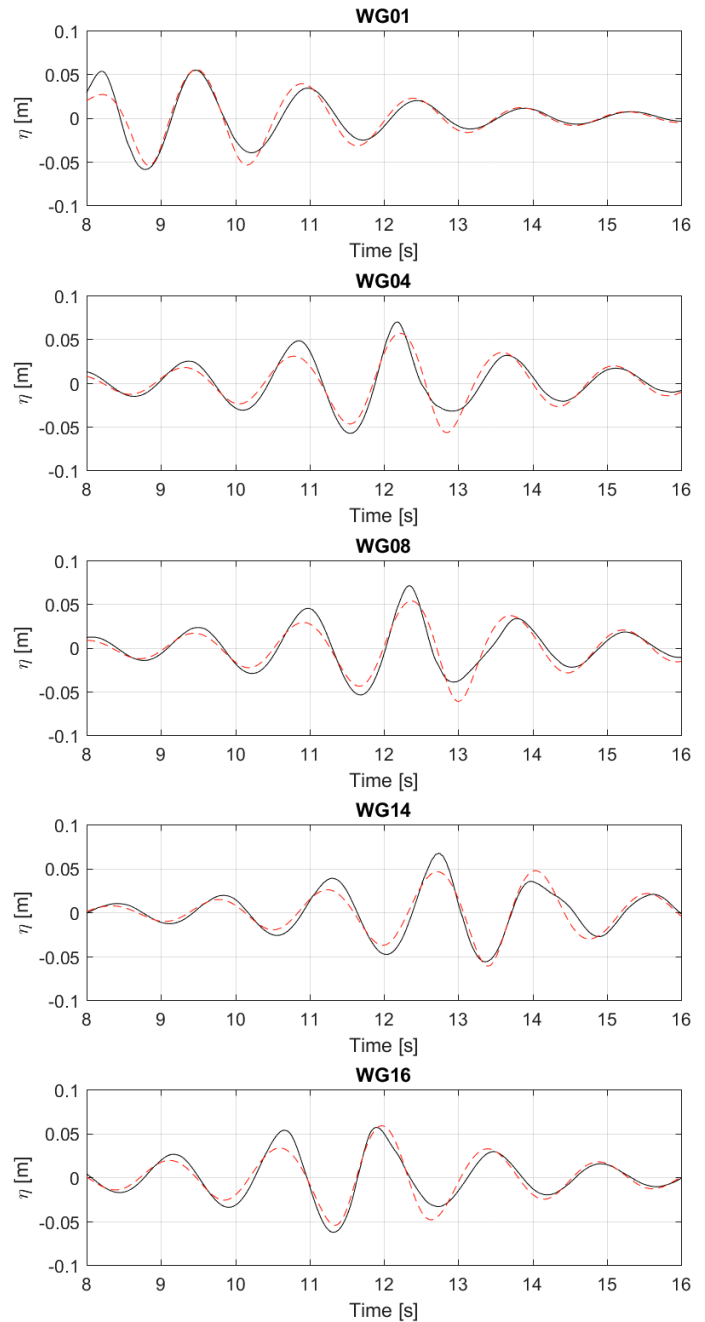

Fig. 3 Comparison of numerical results and experimental data for 11BT1 case. The red curve is from numerical simulation and the black curve is from experiments.
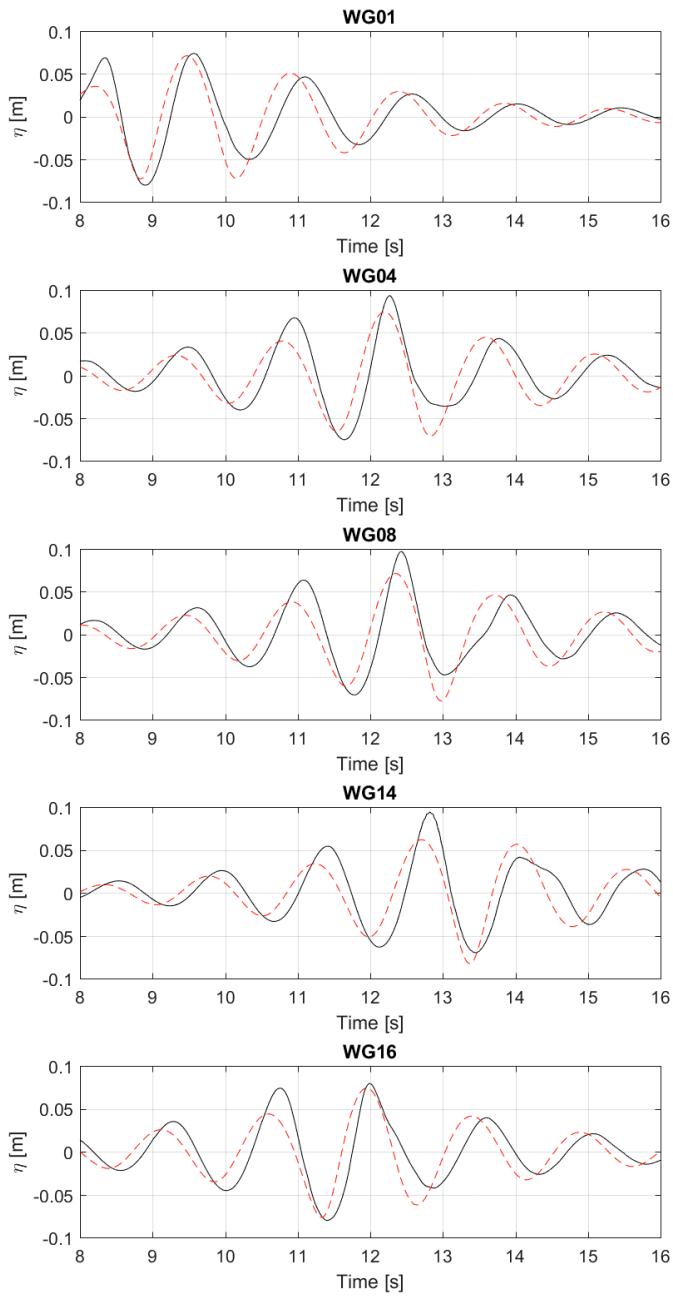
Fig. 4 Same as Fig. 3 but for 12BT1 case.

Results from the numerical wave tank with FPSO in place

In this section, we will focus on the focused wave group interaction with the FPSO-shaped body. We will only present the numerical results below. As mentioned above, as a blind test the experimental data for this part are not available to us currently.

In the experiments, both the surface elevation and the pressure were measured. For the measurement of surface elevation, the positions of the wave gauges were exactly the same as in the empty wave tank. Six pressure sensors were installed at the FPSO to measure the pressure. All the details are given in WSI-CCP website. In the present paper, we will focus on the results that are part of the validity assessment criteria of the blind test, which are the surface elevation at WG 16 (focal position) and the pressure at P3.
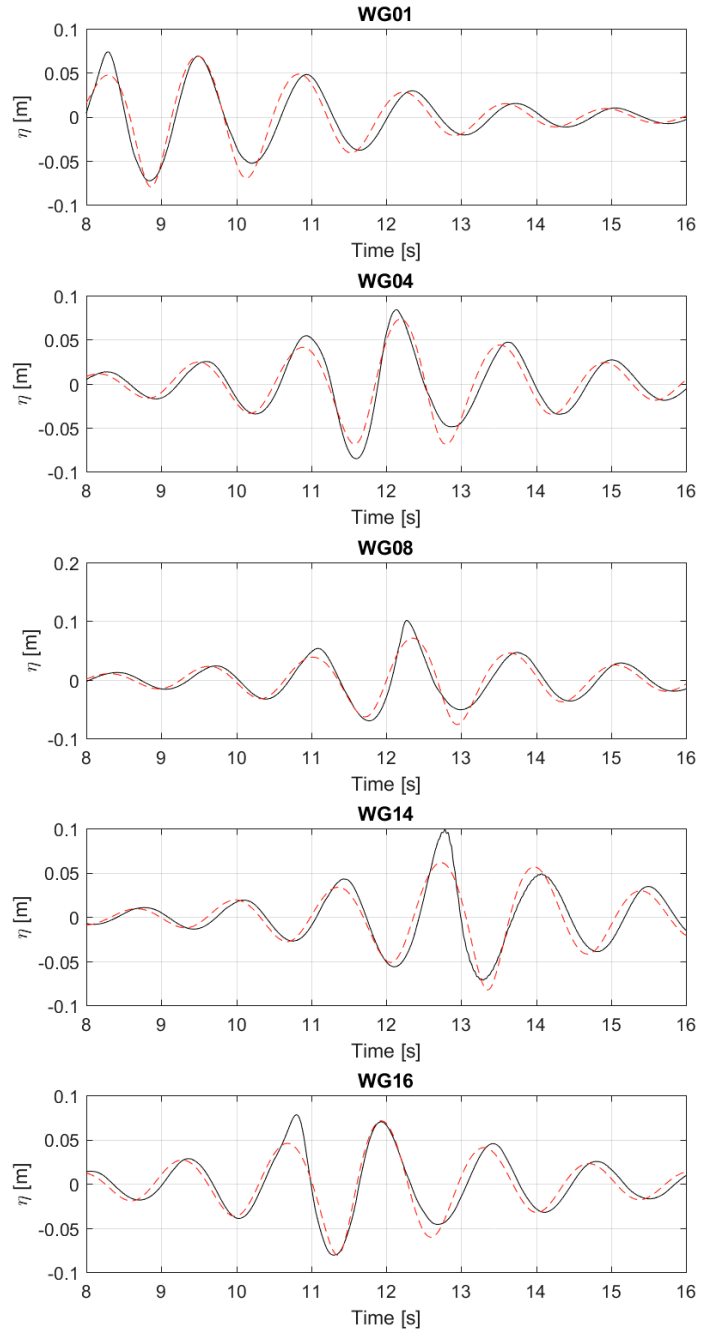

Fig. 5 Same as Fig. 3 but for 13BT1 case.

The surface elevation is given in Fig. 6 for the three cases. The effect of wave steepness is clear which leads to different focal trough height as shown in Fig.6. Fig. 7 shows the time series of pressure. It is seen that around 12 s, the pressure is 0 due to the fact that the free surface is below the pressure sensor, since it is trough-focused wave group. Furthermore, as mentioned above, due to application of Crank-Nicolson scheme, the simulations were not stable enough for case 12BT1. We noticed a sudden increase of pressure at t=15 s due to divergence of the solution of pressure equation. Although it was self-stabilised after this sudden increase, the simulation eventually blew up at around t=17 s, where the time step was reduced to 10^{-17}.

Regarding computational efficiency, the numerical model has relatively

poor performance. The present model was designed for simulation with floating structures. Therefore, the interpolation between two layers of mesh were performed, which took approximately 22 seconds at each time step. Essentially, this significantly slowed down the computation. Typically, for such a case with 20 seconds of simulation time, the actual wall clock time is about 138 hours by using 64 CPUs. This could be several times longer than the time taken by the commonly used interFoam solver.
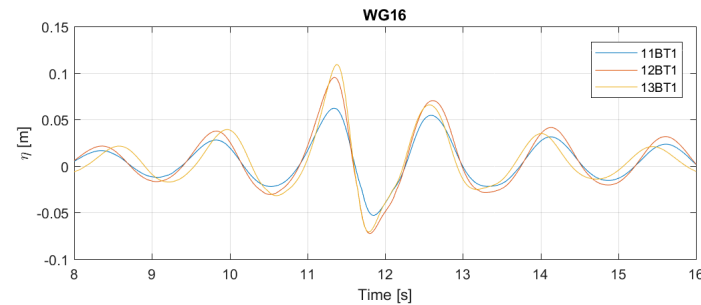

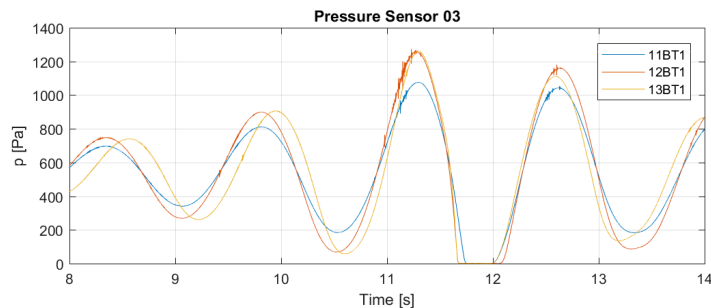Fig. 6 The surface elevation at WG16 for the three cases with FPSO in place.

Fig. 7 The pressure measured at P3 for the three cases with FPSO in place.

CONCLUSIONS

This paper presents the numerical results for the FPSO blind test. The numerical model utilized the overset mesh grid coupled with a boundary condition to generate and absorb waves. The waves were generated based on a second order focused wave theory. The numerical model was first validated against data on wave propagation in empty wave tank. It was concluded that in general, the quality of the generated waves was good. Then we carried out simulations for the cases where an FPSO model was in place. The surface elevation and the pressure on the body were reported here based on the validation criteria.

REFERENCES

Chen, L. F., Zang, J., Hillis, a. J., Morgan, G. C. J., Plummer, a. R. (2014). Numerical investigation of wave–structure interaction using OpenFOAM. *Ocean Eng*, 88, 91–109.

Higuera, P., Lara, J. L., Losada, I. J. (2013). Realistic wave generation and active wave absorption for Navier-Stokes models. Application to OpenFOAM®. *Coastal Eng*, 71, 102–118.

Hu, Z. Z., Greaves, D., Raby, A. (2016). Numerical wave tank study of extreme waves and wave-structure interaction using OpenFoam®. *Ocean Eng*, 126, 329–342.

Mai, T., Greaves, D., Raby, A. and Taylor, P.H. (2016). Physical modelling of wave scattering around fixed FPSO-shaped bodies, *Appl Ocean Res*, Vol. 61, 115-129.

Madsen, P. A., Fuhrman, D. R. (2006). Third-order theory for bichromatic bi-directional water waves. *J Fluid Mech*, 557, 369.

Madsen, P. A., Fuhrman, D. R. (2012). Third-order theory for multi-directional irregular waves. *J Fluid Mech*, 698, 304–334.

Márquez Damián, Santiago. 2013. "An Extended Mixture Model for the Simultaneous Treatment of Short and Long Scale Interfaces." Universidad Nacional Del Litoral.

Ning, D. Z., Zang, J., Liu, S. X., Eatock Taylor, R., Teng, B., Taylor, P. H. (2009). Free-surface evolution and wave kinematics for nonlinear uni-directional focused wave groups. *Ocean Eng*, 36, 15–16.

Paulsen, B. T., Bredmose, H., Bingham, H. B., & Jacobsen, N. G. (2014). Forcing of a bottom-mounted circular cylinder by steep regular water waves at finite depth. *J Fluid Mech*, 755, 1–34.

Zang, J., Gibson, R., Taylor, P. H., Taylor, R. E., Swan, C. (2006). Second order wave diffraction around a fixed ship-shaped body in unidirectional steep waves. *J Offshore Mech Arct Eng*, 128(2), 89-99.